

**INTERNATIONAL JOURNAL OF ENGINEERING SCIENCES & RESEARCH
TECHNOLOGY****INTEGRATED BUCK–FLYBACK NON ISOLATED PFC CONVERTER WITH
CONSTANT ON-TIME CONTROL****Sumy P S**

*M.Tech, Power Electronics, NSS College of Engineering Palakkad, India

ABSTRACT

An integrated buck–flyback non isolated power factor correction converter is proposed in this paper. This new converter is an inherent integration of a buck converter and a flyback converter, which operates in either flyback mode or buck mode according to whether the input voltage is lower or higher than the output voltage. In this way, the dead zones of ac input current in traditional buck power factor correction converter can be eliminated. Therefore, the proposed integrated buck–flyback power factor correction converter can achieve high power factor under universal ac input range, and its input current harmonics can be reduced. Conventional Buck power factor correction converter and proposed converter are simulated using MATLAB/Simulink. A 10W laboratory prototype of the proposed power factor correction converter with 12V input voltage was setup using PIC 16F877 microcontroller. Compared to conventional power factor correction converters, the power factor was improved greatly with the proposed topology especially at low line. This proposed topology is very suitable for high-power non isolated LED drivers with high power factor requirements.

KEYWORDS: AC–DC Converter, Buck–flyback converter, Harmonic currents, Constant On Time(COT)control, High power factor (PF).

INTRODUCTION

AC/DC converter plays a major role in day to-day life. Electrical energy is almost exclusively generated, transmitted and distributed in the form of alternating current. Therefore the question of power factor immediately comes into picture. In recent years, the power electronic systems and devices, which are used more frequently, create harmonic current and pollute the electricity network. Harmonics have a negative effect on the operation of the receiver, which is fed from the same network. AC-DC converters have drawbacks of poor power quality in terms of injected current harmonics, which cause voltage distortion and poor power factor at input ac mains and slow varying ripples at dc output load, low efficiency and large size of AC- DC filters. SMPS, the most frequently used power electronic system, can present nonlinear loads which impose current harmonics onto the main power network. Awareness of the necessity of power quality is increasing, and power factor correction is being implemented on a growing scale.

Power factor correction technique is well applied to the ac/dc converters because it can provide almost sinusoidal input current. Because we want a constant dc supply in the output, so we connect a capacitor in the output of ac/dc converters. This capacitor distorts the input current waveform. To overcome these drawbacks, low harmonic and high power factor converters are used. We replaced the single AC-DC rectifier by a rectifier followed by a DC-DC power factor correction.

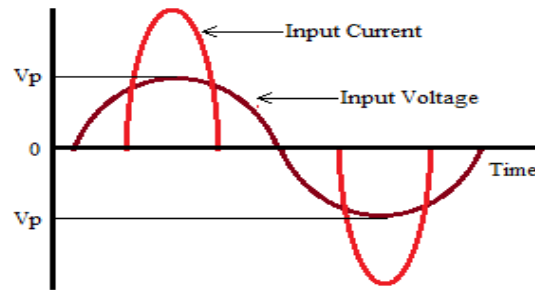


Figure 1. Input waveforms for SMPS with poor power factor

In the past few years, the boost power factor correction converter was the most popular topology due to its inherent shaping ability of the input current. A bridgeless power factor correction boost rectifier, also called dual boost PFC rectifiers is presented in [3]. The boost PFC cannot achieve high efficiency at low line because it works with large duty cycle in order to get high voltage conversion gain. It is hard to increase the power density of boost PFC converter attributes to the thermal problem at low line. With bridgeless structure for boost PFC converter, the efficiency can be improved at low line. But, more components should be added to deal with the electromagnetic interference issue, which leads to high cost. The efficiency improvement of the bridgeless PFC boost rectifier over the conventional PFC boost rectifier is predominantly limited by the on-resistance of the boost switches.

The buck PFC converter can achieve a relatively high efficiency particularly at low input voltage due to the low average input current and rms current, while the voltage stress of the switch is also low. Therefore, the buck PFC converter has drawn much attention. A CRM Buck PFC converter with constant on-time (COT) control is proposed in [6]. Compared to the conventional boost power factor correction converter, the buck PFC converter can achieve high efficiency in the entire universal input voltage range. The buck converter operates in CRM may eliminate the diode reverse-recovery losses, and provide its advantage for ZVS for the turn ON of the switch if the input voltage is lower than double of the output voltage. But there are dead zones in the input current because when the input is lower than output V_O , the converter does not work. The low frequency distortion in the line current arises from its unavoidable notches around the zero crossings of the line voltage, caused by the inability of the buck converter to draw current when the instantaneous input voltage is lower than the output one. So it is difficult for the buck PFC converter to pass the IEC61000-3-2 Class C limits due to the dead zones in the input current which occur when the input voltage is lower than output voltage V_O , as shown in Figure 2.

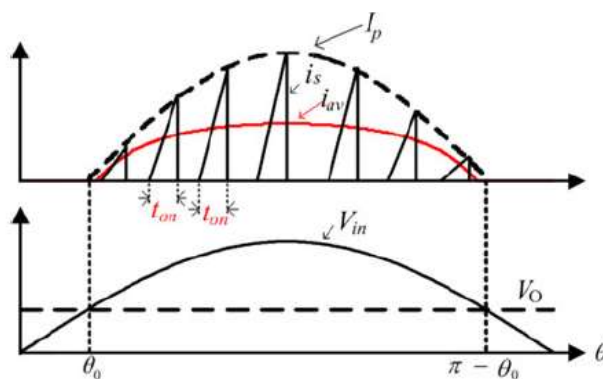


Figure 2. Relationships between input current, switch current, and output voltage with constant on-time control

Another way to improve the PF of the buck PFC converter is to modify the structure of the conventional buck converter. According to this idea, the integrated quadratic buck–boost–buck converter was proposed [8][9]. The paper presents a new non isolated single-stage single-switch high PFC converter suitable for universal input voltage

operation and extreme low output dc voltage applications. This proposed topology eliminate the dead zones of the input current and then achieve high PF. However, the complex structure of this topology makes it unsuitable for actual applications. The buck converter can also be integrated with a flyback converter[10][11][12]. This as a good solution for implementing low-cost high-power-factor ac–dc converters with fast output regulation.

A possible implementation of this principle is, besides the main buck converter, an auxiliary parallel flyback converter feeding the same load, exactly as in Figure 3[13]. This auxiliary power stage is activated only in the interval of the line period in which the main converter is idle and thus can be designed to handle a power which is just a small fraction of the total input power. One of the drawbacks of the solution given is that a complete second power stage is needed, thus increasing the cost of the converter.

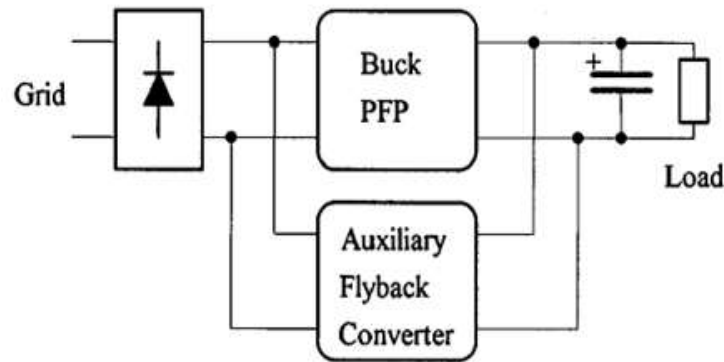


Fig. 3. Schematic of the combined buck-flyback PFC

PROPOSED TOPOLOGY

In conventional buck PFC converter input current waveforms exhibit dead zones at the zero crossing instants of input voltage. This is due to the fact that a buck converter will not draw any current from the input supply when the input voltage less than the output voltage. This will affect the effective utilization of the input power supply. If current absorption is allowed when the input voltage is less than the output voltage maximum power can be drawn from the supply. As we have seen one possible solution for this problem is an integration of flyback converter with buck power factor correction converter.

Proposed integrated buck–flyback non isolated power factor correction converter is derived from a buck converter and a flyback converter. Derivation of the proposed converter is shown in the Figure 4. The structure of the proposed converter is very simple. It is formed by adding two rectifier diodes, one winding of the inductor, and one switch into the conventional buck PFC converter. The source nodes of the added switch Q_2 and the buck switch Q_1 are connected to the ground. The power loops of the buck mode and flyback mode are separated, and no additional component causing losses is added to the power loops. Obviously, the proposed integrated buck–flyback converter can achieve higher efficiency.

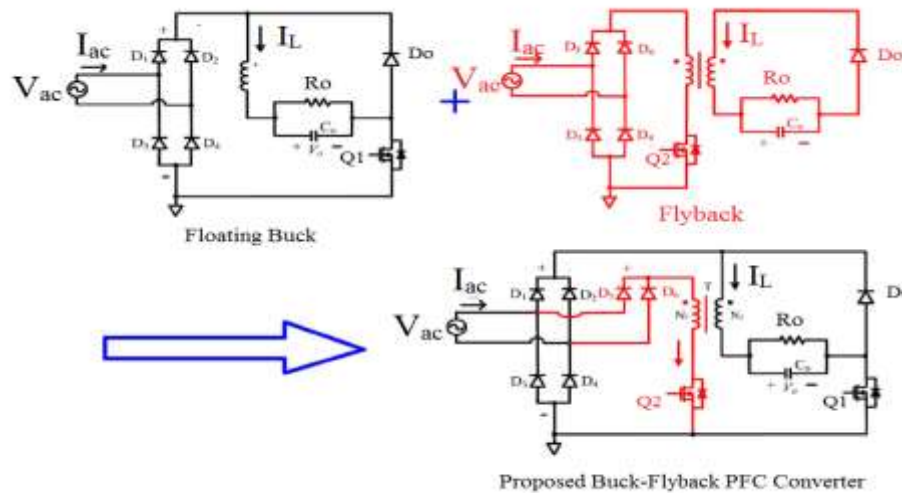


Figure. 4. Derivation of the proposed integrated buck-flyback non isolated PFC converter.

A. Principle of Operation:

There are two different operation modes in a line period for the proposed converter. The proposed converter operates in flyback mode when the input voltage is lower than the output voltage and operates in buck mode when the input voltage is higher than the output voltage. Thus a current can be drawn from the supply even when the main buck converter is idle. In this way, there are no dead zones in the input current of the proposed converter. Therefore, it can achieve high power factor and pass the IEC61000-3-2 Class C limits easily. An improved Constant On Time (COT) control is applied to the proposed integrated Buck-Flyback power factor correction converter and forces it to operate in critical conduction mode (CRM).

In COT control, although the switching period is variable, the on time of one switching cycle of the switch is almost constant in one line cycle. The peak current value is a function of the input voltage as described in (1).

$$\frac{V_{in}-V_{out}}{L} = I_p \tag{1}$$

where V_{in} is the rectified input supply voltage, V_o is output voltage across the output capacitor, L is the inductance of the transformer secondary winding, T_{on} is the ON duration of the switch and I_p is the peak value of the input current in the working region. From (1) inductance L and input supply voltage are constants. V_o is kept almost constant by using a large value of output capacitance. If T_{on} is kept constant from (1) it is clear that I_p will be proportional to V_{in} .

Accordingly, the peak current in working region can follow the input voltage, when output voltage V_o is constant. That means the input voltage and input current will be in phase and sinusoidal. Thus the power factor of the input will get improved with the proposed integrated Buck- Flyback power factor correction converter.

B. Proposed Control Strategy:

A constant on time control strategy is adopted which a sinusoidal input current that follows the input voltage waveform. The proposed converter is operated in Critical Conduction Mode thus ensures Zero Current Switching which reduces the switching losses. Circuitry for the improved Constant On Time (COT) control is shown in the Figure 5. The output current is detected for constant output current control of the LED load.

The control signal V_{ph} is the result of the magnitude comparison between V_{in} and $V_{boundary}$. V_{ph} is high logic when V_{in} is larger than $V_{boundary}$ and vice versa. The driving signals V_{G1} and V_{G2} are controlled by V_{ph} for the different operation modes alternately. The current zero crossing detection signal generated by the auxiliary winding of transformer T can be applied to both of the flyback and buck modes. As shown in Figure 5, the control signal V_{ph} is the result of the magnitude comparison between V_{in} and $V_{boundary}$. V_{ph} is high logic when V_{in} is larger than $V_{boundary}$ and vice

versa. The driving signals V_{G1} and V_{G2} are controlled by V_{ph} for the different operation modes alternately. The current zero crossing detection signal generated by the auxiliary winding of transformer T can be applied to both of the flyback and buck modes.

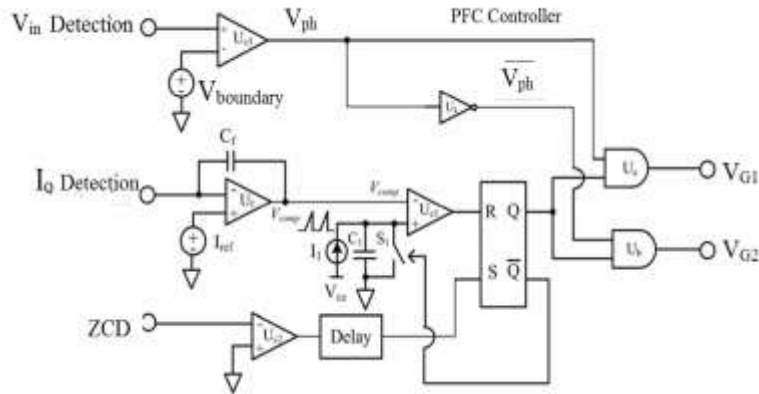


Figure 5. Improved Constant On Time control Scheme

Some key waveforms are shown in Figure 6. The proposed integrated buck–flyback non isolated PFC converter operates in buck mode when V_{ph} is in high logic level, while it operates in flyback mode when V_{ph} is in low logic level. Transition processes between those two modes are natural.

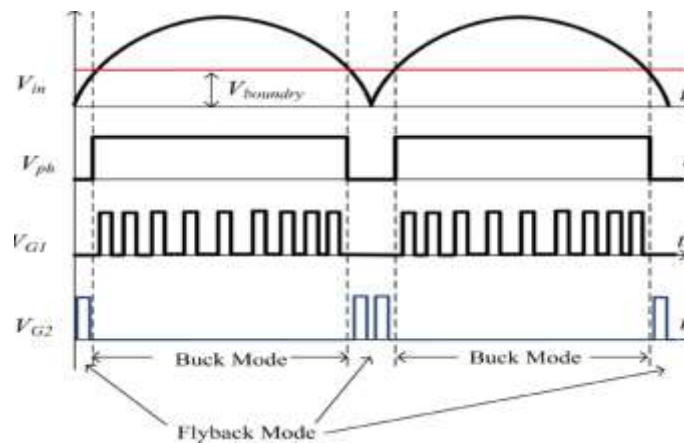


Figure 6. Key waveforms in COT control diagram.

C. Operation Stages:

The operation process of the proposed converter in a line period can be divided into 12 operation stages, 6 for positive half cycle and 6 for negative half cycle.

i. Positive Half Cycle of AC input:

When the input voltage V_{ac} is positive and the magnitude of V_{ac} is smaller than V_o , the proposed converter operates in flyback mode. In this mode, switch Q_1 keeps off, and switch Q_2 keeps switching. There exist three stages when the proposed converter operates in this mode.

Stage 1: Before this stage, the output diode D_o carries the output current, and switch Q_2 is off. Once the current flowing through D_o falls to zero, D_o turns off, and the equivalent capacitor of switch Q_2 is resonant with the magnetizing inductor of the transformer T , as shown in Figure 7(a)

Stage 2: When the voltage across the auxiliary winding of the transformer T falls to zero, the output of comparator U_{c2} flips from a low voltage level to a high voltage level. After a delay time, switch Q_2 is turned on at the valley of $V_{DS_{Q2}}$. The primary magnetizing inductor of transformer T is charged by V_{ac} through D_5 and D_4 , as shown in Figure 7(b)

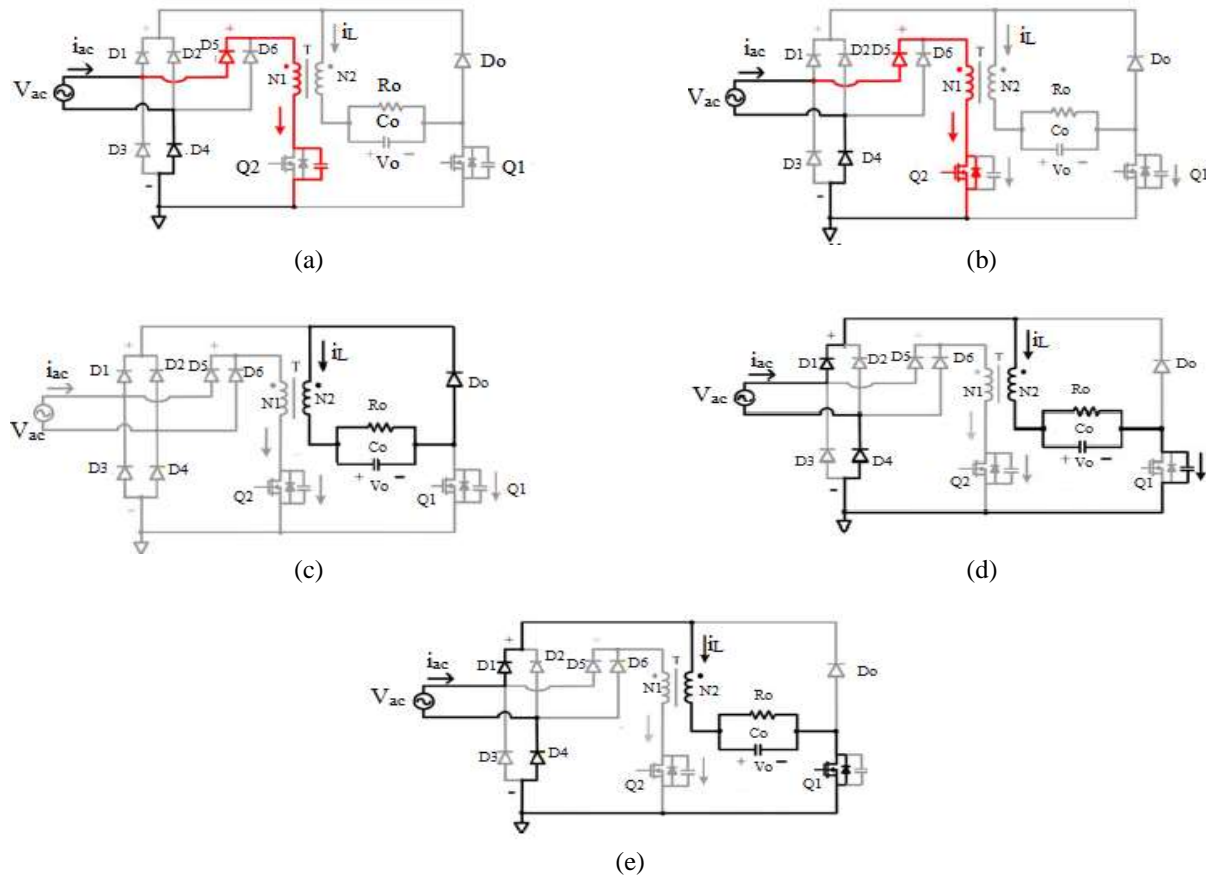


Fig. 7. Equivalent circuits of the proposed converter for positive half cycle

Stage 3: When switch Q_2 is off, the secondary magnetizing inductor of transformer T is discharged by V_o through D_o on the secondary side of the transformer, as shown in Figure 7(c).

When the input voltage V_{ac} is positive and the magnitude is larger than V_o , the proposed converter operates in buck mode. In this mode, switch Q_2 keeps off, and switch Q_1 keeps switching. There also exist three stages when the proposed converter operates in this mode.

Stage 4: Before this stage, the output diode D_o carries the output current, and switch Q_1 is off. Once the current flowing through D_o falls to zero, D_o turns off, and the equivalent capacitor of switch Q_2 is resonant with the magnetizing inductor of the transformer, as shown in Figure 7(d).

Stage 5: When the voltage across the auxiliary winding of the transformer falls to zero, the output of comparator U_{c2} flips from a low voltage level to a high voltage level. After a delay time, switch Q_1 is turned on at the valley of

$V_{DS_{Q1}}$. The secondary magnetizing inductor of transformer T is charged by $V_{ac} - V_o$ through D_1 and D_4 , as shown in Figure 7(e).

Stage 6: When switch Q_1 is off, the secondary magnetizing inductor of transformer T is discharged by V_o through D_o as shown in the Figure 7(c).

ii. *Negative Half Cycle of AC Input:*

When the input voltage V_{ac} is negative, the proposed converter also operates in flyback mode and buck mode in different input voltage regions. The operation processes in negative half-cycle of ac input can also be divided into six operation stages, and the equivalent circuits are shown in Figure 8(a) to 8(d). The operation processes of the proposed converter in the negative half-cycle of ac input are similar to those of the positive half-cycle.

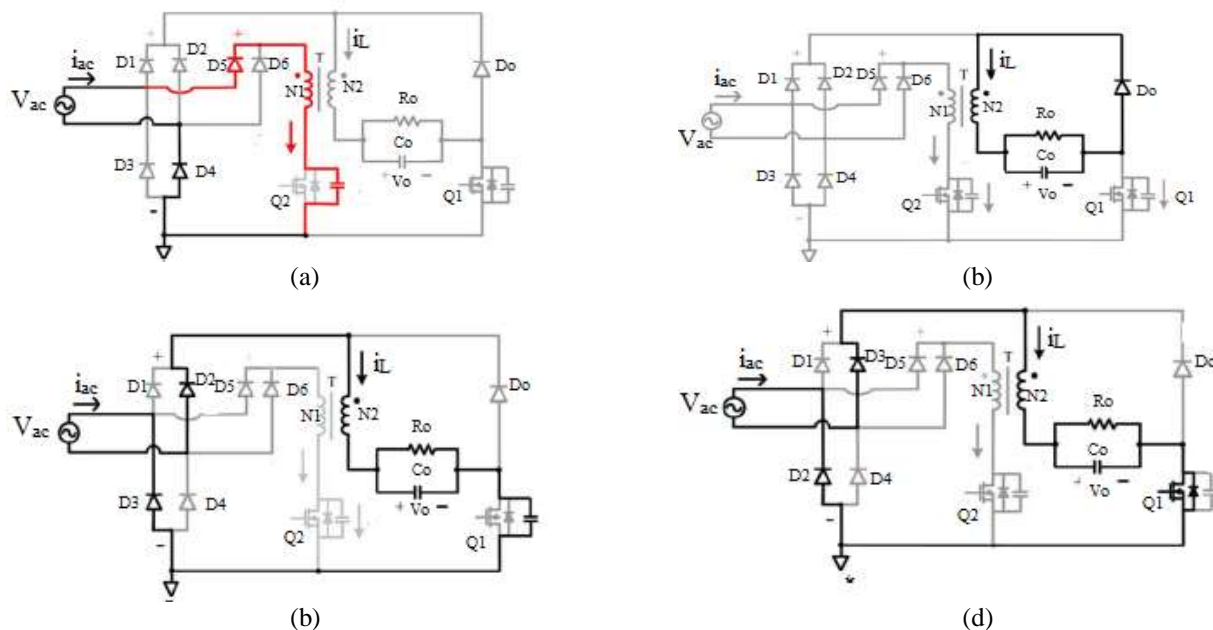


Fig. 8. Equivalent circuits of the proposed converter for negative half cycle

DESIGN CONSIDERATIONS

Input Current Analysis:

When the input voltage is lower than the output voltage in half line cycle, the buck converter does not work. The conduction angle of the input current during buck mode equals $(\pi - 2\theta_0)$. Assuming V_{im} is the amplitude of the line voltage, then, angle θ_0 is defined as

$$\begin{aligned} \theta_0 &= \arcsin(V_{boundary}/V_{im}) \\ \theta_0 &= \arcsin(V_o/V_{im}) \end{aligned} \tag{1}$$

When the input voltage is higher than the output voltage, the buck converter begins working, and the slope of the inductor current i_{L_s} for the buck operating region in half line cycle is given by the expression

$$L di_{L_s}(t)/dt = V_{im} |\sin(\theta)| - V_o, \quad \theta \in (\theta_0, \pi - \theta_0) \tag{2}$$

where $\theta = \omega_l t$ and $\omega_l = 2\pi f_l$ is the line angular frequency. So, the peak value of the inductor current during switching cycle during buck mode can be modified as follows:

$$I_{pk1}(\theta) = (V_{im} |\sin(\theta)| - V_o) T_{on} / L_s \tag{3}$$

where L_s in the secondary winding inductance and T_{on} is the on-time of the switch, which is almost constant during half line cycle. The peak value of the inductor current during switching cycle during flyback mode can be written as follows:

$$i_{pk2}(\theta) = (V_{im} \cdot \sin \theta) T_{on} / L_p \quad (4)$$

where L_p in the primary winding inductance

$$D(\theta) = V_o / (V_{im} |\sin(\theta)|), \quad \theta \in (\theta_0, \pi - \theta_0) \quad (5)$$

Then, the average input current i_{av} of the buck converter is determined as follows:

$$i_{av}(\theta) = I_{pk1}(\theta) D(\theta) / 2, \quad \theta \in (\theta_0, \pi - \theta_0) \quad (6)$$

Output Voltage Selection:

Within a half line cycle, the input current can flow only when the input voltage is greater than the output voltage. It should be noted that the PF is affected by the output voltage significantly. With an increasing output voltage, the PF decreases. Although lower output voltage results in higher PF, the efficiency of buck converter will decrease with the decrease of output voltage at same load. The output voltage is preferred to be set around 80 V considering the voltage stress of the output capacitor

Inductance Selection:

The input power P_{in} is calculated as follows:

$$P_{in} = \frac{2}{\pi} \int_{\theta_0}^{\pi/2} i_{av}(\theta) V_{im} \cdot \sin \theta \, d\theta \quad (7)$$

Assuming η is the efficiency of the converter, the output power P_o can be expressed as follows:

$$P_o = \eta \cdot P_{in} = \frac{2\eta}{\pi} \int_{\theta_0}^{\pi/2} i_{av}(\theta) \cdot V_{im} \cdot \sin \theta \, d\theta \quad (8)$$

By substituting (6) into (8) we will get

$$P_o = \eta \cdot P_{in} = \frac{\eta T_{on}}{\pi L_s} \int_{\theta_0}^{\pi/2} (V_{im} \cdot \sin \theta - V_o) \cdot V_o \, d\theta \quad (9)$$

During buck mode,

$$T_{off}(\theta) = \frac{I_{pk1}(\theta) \cdot L}{V_o} \quad (10)$$

Switching frequency as a function of time is given by,

$$f_s(\theta) = 1 / (T_{on} + T_{off}(\theta)) = V_o / (T_{on} \cdot V_{im} \sin(\theta)) \quad (11)$$

From (9) T_{on} can be expressed as

$$T_{on} = \frac{\pi L_s P_o}{\eta} \frac{1}{\int_{\theta_0}^{\pi/2} (V_{im} \cdot \sin \theta - V_o) \cdot V_o \, d\theta} \quad (12)$$

Combining (11) and (12),

$$f_s = \frac{\eta \cdot V_o^2}{\pi \cdot L_s \cdot P_o \cdot V_{im} \cdot \sin \theta} \int_{\theta_0}^{\pi/2} (V_{im} \cdot \sin \theta - V_o) \, d\theta, \quad \theta_0 \leq \theta \leq \pi - \theta_0 \quad (13)$$

Obviously, the lowest frequency in half line cycle appears at $\theta = \pi/2$. Therefore, the minimum frequency as a function of input voltage V_{im} can be obtained when $\theta = \pi/2$

$$f_{s-\min} = \frac{\eta \cdot V_o^2}{\pi \cdot L_s \cdot P_o \cdot V_{im-\min}} \int_{\theta_o}^{\pi/2} (V_{im-\min} \sin\theta - V_o) d\theta \quad (14)$$

Then, the transformer secondary winding inductance L_s is obtained as follows:

$$L_s = \frac{\eta \cdot V_o^2}{\pi \cdot f_{s-\min} \cdot P_o \cdot V_{im-\min}} \int_{\theta_o}^{\pi/2} (V_{im-\min} \sin\theta - V_o) d\theta \quad (15)$$

where $V_{im-\min} = 60$. If the minimum switching frequency $f_{s-\min}$ is assumed to be 10 kHz, output power is designed at 100W and the output voltage is designed at 60V. Then,

$$\theta_o = \arcsin (V_o/V_{im})$$

where V_{im} is 100V. θ_o is obtained as,

$$\theta_o = 0.2\pi$$

For an efficiency η of 0.96, the inductance is obtained as,

$$L_s = 1 \text{ mH.}$$

$$L_p/L_s = (N_1/N_2)^2 \quad (16)$$

where N_1/N_2 is the turns ratio which can be taken as n . Choosing n as 2.

$$L_p = 4 \text{ mH}$$

Output Capacitance Selection:

Output capacitor is designed by the equation,

$$C_f = \frac{I_o}{8f_s \cdot \Delta V_{Cf}} \quad (17)$$

where ΔV_{Cf} is usually considered as 5%–10% of the output voltage. This capacitor value is chosen to be higher than the one given by the above equation and

$$I_o = P_o/V_o$$

$$C_f = 150 \mu\text{F}$$

SIMULATION RESULTS

The performance of the proposed converter and the control strategy are evaluated by conducting the Simulation analysis. MATLAB/Simulink version R2012a is used for simulation. The input given is 100 V and the parameters are designed for a 100 W, 60V topology.

Table 1. Simulation Parameters For Integrated Buck- Flyback Converter

PARAMETER	VALUE
L_p	1mH
L_s	4mH
Transformer Turns ratio, n	2
Output Capacitor, C_o	150 μ F
Switch Q_1, Q_2	IRF 840
Diode D_o	1N4007

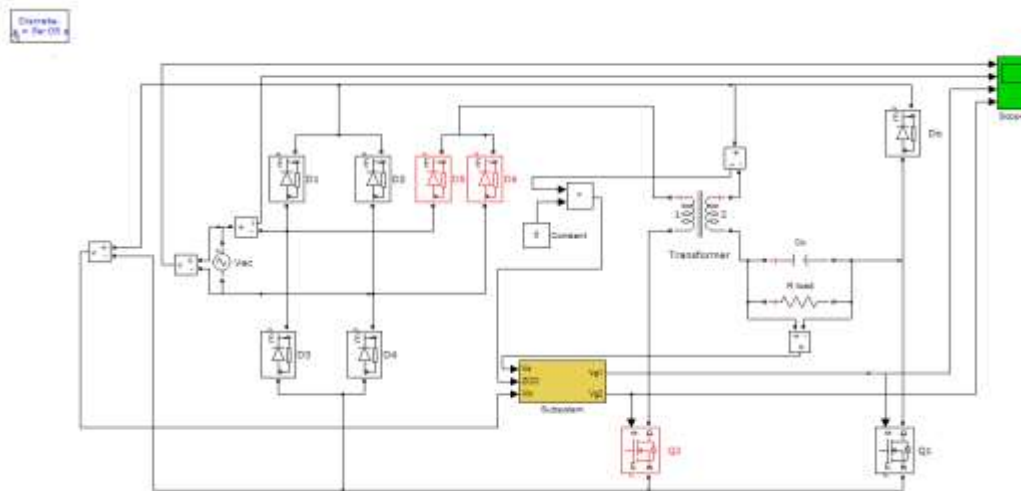


Fig. 9. Proposed Converter Circuit

Matlab Simulation circuit for the proposed converter is shown in figure 9. Matlab Simulation circuit for the COT Controller for Proposed Converter is shown in figure 10. Figure 11 shows the Input voltage and Input current waveforms of buck PFC converter. Figure 12 shows the Input voltage and Input current waveforms of proposed integrated buck-flyback PFC converter obtained from simulation.

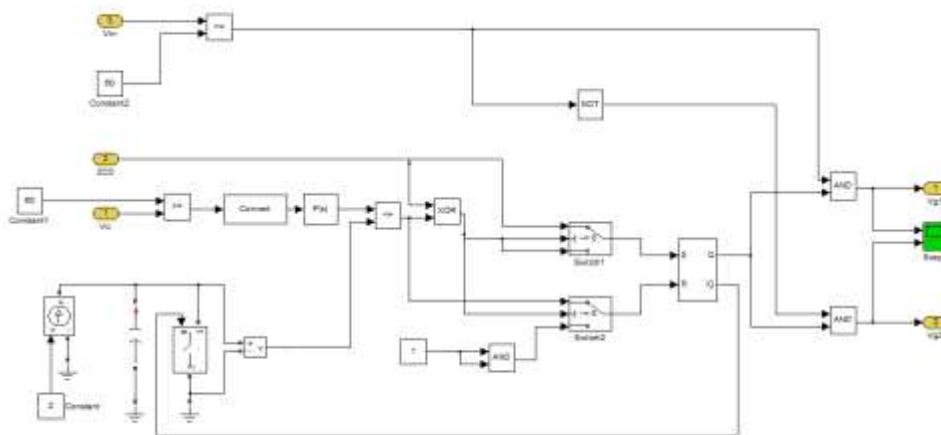


Fig. 10. COT Controller for Proposed Converter

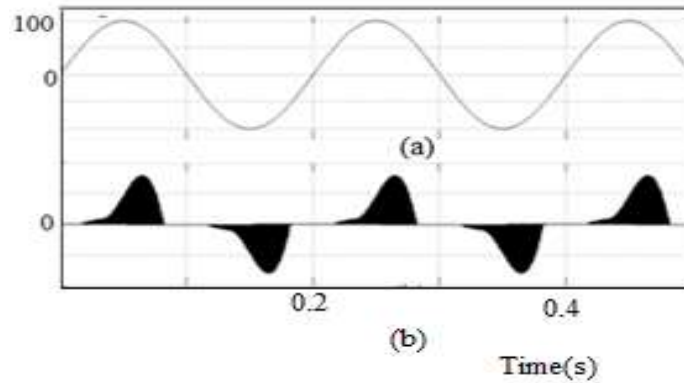


Fig. 11. Input voltage, Input current and Inductor Current of buck PFC converter at 100 V

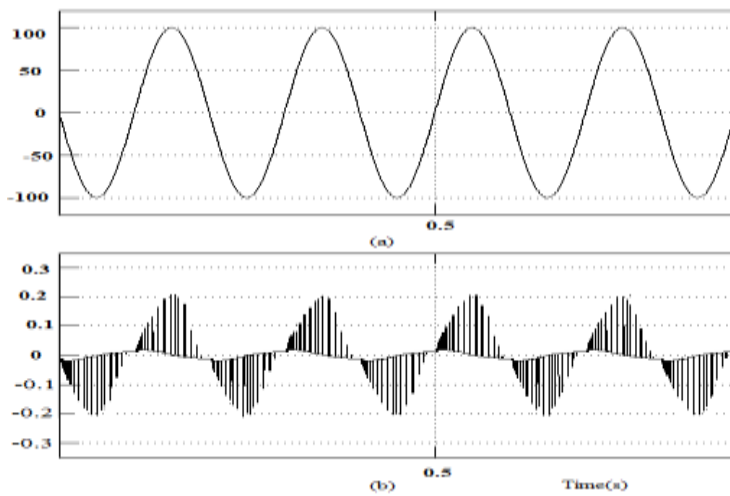


Fig. 12 Input voltage and Input current of proposed PFC converter at 100 Vac

From fig.11 and fig.12 it is clear that the dead zone in the input current waveform is very much reduced in proposed buck-flyback PFC converter. Also the input current is almost sinusoidal and the phase difference between the voltage and current is very much reduced

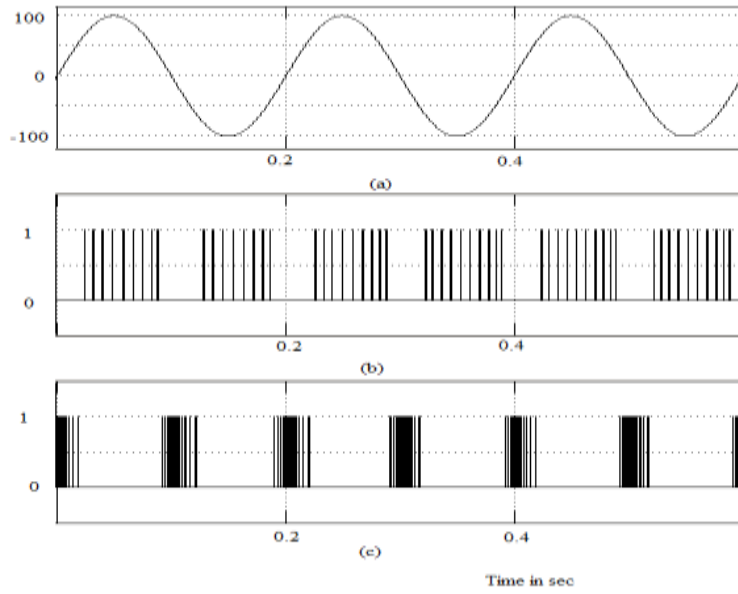


Fig. 13. Input Voltage and generated switching Signals V_{g1} and V_{g2}

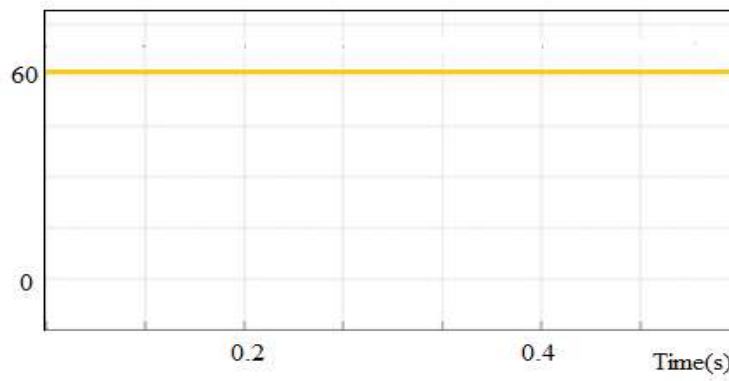


Fig. 14. Output Voltage for 100 V_{ac}

EXPERIMENTAL RESULTS

Laboratory setup of the proposed Buck-Flyback converter prototype with 12V input supply is shown in Figure 15. A step down transformer was used to step down the input 230V to 12V input. PIC 16f877 microcontroller was used to generate the control signals for the buck and flyback switches.



Fig. 15. Laboratory Setup

CONCLUSION


An integrated non isolated buck–flyback PFC converter topology has been proposed in this paper. The structure of this topology is simple, and both of the switches are easy to drive. The proposed converter operates in flyback mode when the input voltage is lower than the output voltage and operates in buck mode when the input voltage is higher than the output voltage. In this way, there will not be any dead zones in the input current of the proposed converter. Therefore it can achieve high power factor and pass the IEC61000-3-2 Class C limits easily. Conventional Buck PFC converter and proposed converter are simulated using MATLAB/Simulink. A 10W laboratory prototype of integrated Buck-flyback power factor correction converter with 12V input voltage was setup. PIC 16F877 is used to generate controlled switching signals for buck and flyback switches. Compared to conventional PFC topologies obviously the proposed converter can improve the PF greatly particularly at low line voltage. This topology could achieve high PF of 0.96. This proposed topology is very suitable for high-power non isolated LED drivers with high PF requirements. The proposed integrated nonisolated buck–flyback PFC converter topology can also be extended to isolated topology by replacing the buck part with an isolated buck-type topology such as forward converter.

REFERENCES

- [1]. Y. Jang and M. M. Jovanovi'c, "Bridgeless high-power-factor buck converter," *IEEE Trans. Power Electron.*, vol. 26, no. 2, pp. 602–611, Feb. 2011.
- [2]. C.-Y. Chiang and C.-L. Chen, "Zero-voltage-switching control for a PWM buck converter under DCM/CCM boundary," *IEEE Trans. Power Electron.*, vol. 24, no. 9, pp. 2120–2126, Sep. 2009.
- [3]. L. Huber, J. Yungtaek, and M. M. Jovanovi'c, "Performance evaluation of bridgeless PFC boost rectifiers," *IEEE Trans. Power Electron.*, vol. 23, no. 3, pp. 1381–1390, Mar. 2008.
- [4]. M. Mahdavi and H. Farzanehfard, "Bridgeless SEPIC PFC rectifier with reduced components and conduction losses," *IEEE Trans. Ind. Electron.*, vol. 58, no. 9, pp. 4153–4160, Sep. 2010.
- [5]. Xiaogao Xie, Chen Zhao, Lingwei Zheng and Shirong Liu "An Improved Buck PFC Converter With High Power Factor", *IEEE Transactions On Power Electronics*, Vol. 28, No. 5, May 2013
- [6]. X. Wu, J. Yang, J. Zhang, and M. Xu, "Design considerations of a high efficiency soft-switched buck AC–DC converter with constant on-time (COT) control," *IEEE Trans. Power Electron.*, vol. 26, no. 11, pp. 3144–3152, Nov. 2011
- [7]. J. Yang, J. Zhang, X. Wu, Z. Qian, and M. Xu, "Performance comparison between buck and boost CRM PFC converter," in *IEEE Proc. 12th Workshop Control Model. Power Electron. (COMPEL)*, Jun. 2010, pp. 1–5.

- [8]. M. A. Al-Saffar, E. H. Ismail, and A. J. Sabzali, "Integrated buck–boost quadratic buck PFC rectifier for universal input applications," *IEEE Trans. Power Electron.*, vol. 24, no. 12, pp. 2886–2896, Dec. 2009.
- [9]. J. Marcos Alonso, J. Viña, D. Gacio, L. Campa, G. Martinez, and R. Osorio, "Analysis and design of the quadratic buck–boost converter as a high-power-factor driver for power-LED Lamps," in *Proc. IEEE IECON*, Glendale, AZ, 2010, pp. 2541–2546
- [10]. J. M. Alonso, M. A. D. Costa, and C. Ordiz, "Integrated buck–flyback converter as a high-power-factor off-line power supply," *IEEE Trans. Ind. Electron.*, vol. 55, no. 3, pp. 1090–1100, Mar. 2008.
- [11]. M. A. Dalla Costa, J. M. Alonso, J. C. Miranda, J. Garcia, and D. G. Lamar, "A single-stage high-power-factor electronic ballast based on integrated buck flyback converter to supply metal halide lamps," *IEEE Trans. Ind. Electron.*, vol. 55, no. 3, pp. 1112–1122, Mar. 2008
- [12]. Gacio, J. M. Alonso, A. J. Calleja, J. García, and M. Rico-Secades, "Universal-input single-stage high-power-factor power supply for HBLEDs based on integrated buck–flyback converter," *IEEE Trans. Ind. Electron.*, vol. 58, no. 2, pp. 589–599, Feb. 2011.
- [13]. G. Spiazzi and S. Buso, "Power factor preregulators based on combined buck–flyback topologies," *IEEE Trans. Power Electron.*, vol. 15, no. 2, pp. 197–204, Mar. 2000.

AUTHOR BIBLIOGRAPHY

	<p>Sumy P S Received B. Tech degree in Electrical and Electronics Engineering from Government Engineering College, Idukki, Kerala, India. and M.Tech in power Electronics from NSS College of Engineering Palakkad, Kerala, India</p>
------------------------------------------------------------------------------------	--------------------------------------------------------------------------------------------------------------------------------------------------------------------------------------------------------------------------------------------------